



Elastocaloric cooling of shape memory alloys: A review

Junyu Chen, Liping Lei, Gang Fang*

State Key Laboratory of Tribology, Department of Mechanical Engineering, Tsinghua University, Beijing 100084, China

ARTICLE INFO

Keywords:

Elastocaloric effect
Shape memory alloy
Solid-state cooling
Martensitic transformation
Cooling prototype

ABSTRACT

Elastocaloric cooling technology based on shape memory alloys (SMAs) exploits the caloric effect generated by stress-induced phase transformation of elastocaloric materials to realize refrigeration. It is characterized by eco-friendliness, high efficiency and energy saving and thus has been considered as one of the most promising candidates to replace the conventional vapor-compression cooling technology. Compared with magnetocaloric, electrocaloric and barocaloric refrigeration technologies, elastocaloric cooling balances cost, refrigeration capacity and efficiency, and feasibility. The review presents an overview of elastocaloric cooling from the fundamentals to the device design. We firstly describe the thermodynamic fundamentals and the characterization methods of the elastocaloric effect. Secondly, the research progress and the challenges in NiTi-based, Cu-based, Fe-based, and ferromagnetic SMAs as elastocaloric refrigerants are summarized. Furthermore, the development and the application prospects of high-performance elastocaloric materials are proposed. Finally, the advance of elastocaloric cooling prototypes is also analyzed and discussed. This review tries to outline the open crucial questions and to provide an insight to the community for further investigations of clean elastocaloric cooling.

1. Introduction

Refrigeration has become an indispensable technology in modern society for food and medicine preservation, cold-chain transportation, and space cooling in residence and industry [1]. Currently, the mainstream cooling technology is still the old vapor-compression technology, which harvests the latent heat from the gas-liquid transformation of chemical refrigerants to achieve refrigeration. However, the excessive use of chemical refrigerants has brought severe environmental impacts such as ozone layer depletion and global warming [2,3]. Besides, refrigeration consumption has accounted for about 20% of the global electricity usage nowadays [4]. Worldwide refrigeration requirement is projected to triple by 2050 owing to the growing populations and living standards, and global warming [5]. Therefore, it is of both academic and practical significance to develop novel cooling technologies with environmental protection and energy saving to replace the hazardous and unsustainable vapor-compression-based refrigeration.

Solid-state cooling technologies operated with green refrigerants provide an unprecedented opportunity to mitigate the energy crisis and environmental issues facing human beings [6]. The caloric effects of materials are activated by external stimuli to realize cooling. Caloric materials can be classified into magnetocaloric, electrocaloric, barocaloric and elastocaloric when the caloric effect is induced by magnetic

field, electric field, hydrostatic pressure and uniaxial stress, respectively [7]. Magnetocaloric cooling with more than 100 prototypes is the most matured and in-depth research among solid-state refrigeration technologies [8] and shows great potential in low-temperature refrigeration [9]. However, its operation requires a huge magnetic field coupled with complex structures, high cost and large size, which greatly hinders its wide application. Electrocaloric materials, mainly polymers and ceramics, have to be processed in the form of thin films in order to generate strong electric fields to motivate perceptible caloric effects, thus dielectric breakdown often brings material failure [10]. Besides, the low efficiency of electrocaloric cooling is dissatisfaction [6]. Barocaloric materials normally only have a weak caloric effect and the corresponding complex driving field (hydrostatic pressure) limits the subsequent heat transfer [6,11]. If such shortcomings could be overcome, barocaloric cooling might have a bright future. Compared with the aforementioned solid-state refrigeration technologies, elastocaloric cooling of shape memory alloys (SMAs) has the advantages of significant caloric effect and simple actuation, as shown in Table 1. Therefore, elastocaloric cooling has the greatest potential as an alternative to the conventional vapor-compression technology among crowded candidates [3].

Elastocaloric materials undergoing cyclic diffusionless transformation play a key role in energy conversion and transfer,

* Corresponding author.

E-mail address: fangg@tsinghua.edu.cn (G. Fang).

Table 1

Adiabatic temperature change ΔT_{ad} , isothermal entropy change ΔS_{iso} and driving fields for typical calorific materials.

Caloric material	Temperature change $ \Delta T_{ad} $ (K)	Entropy change $ \Delta S_{iso} $ (J kg ⁻¹ K ⁻¹)	Field change	Ref.
Elastocaloric				
(Ni ₅₀ Mn _{31.5} Ti _{18.5}) _{99.8} B _{0.2}	31.5	45	700 MPa	[17]
Ni _{48.5} Ti _{51.1}	25	35	900 MPa	[24]
Ti ₅₀ Ni ₄₄ Cu ₅ Al ₁	25	53.5	600 MPa	[16]
Cu _{68.1} Zn _{15.8} Al _{16.1}	6	21	120 MPa	[25]
Magnetocaloric				
Gd	13	11	5 T	[26]
Gd ₅ Si ₂ Ge ₂	15	19	5 T	[27]
LaFe _{11.4} Mn _{0.4} Si _{1.5}	3	11	1.2 T	[28]
MnFe _{0.95} P _{0.05} Si _{0.33}	2.6	10	1 T	[29]
Electrocaloric				
PbZr _{0.46} Sn _{0.45} Ti _{0.1} O ₃	1.6	...	30 kV cm ⁻¹	[30]
P(VDF-TrFE)	12	...	1200 kV cm ⁻¹	[31]
PbZr _{0.95} Ti _{0.05} O ₃	12	...	480 kV cm ⁻¹	[32]
Barocaloric				
Gd ₅ Si ₂ Ge ₂	1.1	11	200 MPa	[33]
LaFe _{11.3} Co _{0.5} Si _{1.2}	2.2	8.7	200 MPa	[34]
Ni ₄₉ Mn ₃₆ In ₁₅	4.5	24.4	260 MPa	[35]

refrigeration capacity and efficiency, and structural stability of solid-state cooling. So far, the reported elastocaloric refrigerants mainly include NiTi-based, Cu-based, Fe-based, and ferromagnetic SMAs, which have their unique advantages and drawbacks [12]. Considerable efforts surrounding latent heat, stability, fatigue life, working temperature window and cooling efficiency have been devoted to improving cooling performances of elastocaloric materials by controlling chemical composition or microstructure [13–17]. In general, the materials optimized by the above methods usually only enhance partial performances but at the expense of other indicators, namely, latent heat, transformation hysteresis, stability, fatigue life, working temperature window and cooling efficiency are often mutually restricted [18,19]. In addition, the development of elastocaloric devices is blooming with interdisciplinary collaboration [20–23]. This review summarizes the latest research progress of elastocaloric cooling and also sheds light on the opportunities and challenges, which might push a significant step forward towards the commercialization of such energy-efficient and environment-friendly refrigeration technology.

2. Elastocaloric effect and thermodynamic fundamentals

2.1. Elastocaloric effect

In 1805, the elastocaloric effect (eCE) was first reported by British blind natural philosopher Gough, who detected the temperature change

of the rapidly stretched rubber by his lips [36]. Shortly afterwards, Thomson suggested a thermodynamic interpretation [37] and various elastocaloric materials were discovered by Joule [38]. However, due to the weak calorific effects of common metals and polymers, eCE rarely receives attention in the following over 100 years. Until 1980, Rodriguez and Brown occasionally discovered a significant eCE in Cu_{69.6}Al_{27.7}Ni_{2.7} SMA during studying martensitic transformation [39]. In 2004, Quarini and Prince reported giant temperature variations of 16 K and -14 K in the NiTi alloy subjected to a loading-holding-unloading protocol and originally proposed the concept of solid-state cooling [40]. Since then, the research of solid-state cooling based on SMAs was blossoming.

The eCE of SMAs is derived from the release and absorption of latent heat in the forward and reverse martensitic transformation during cyclic loading and unloading [40]. Fig. 1 visualizes the eCE of NiTi SMA in a Brayton cycle with four steps: (i) The adiabatic loading triggers an exothermic martensitic transformation from the austenite phase with a high-symmetry cubic lattice to the martensite phase with a low-symmetry monoclinic lattice (Stage 1 to Stage 2) and heats up the material. (ii) During the holding stage, the applied stress or strain is kept constant (Stage 2 to Stage 3). In the meantime, the heated material releases heat to the ambient and thus returns to room temperature. This step can be utilized to heating. (iii) The applied loading is adiabatically removed, an endothermic reverse martensitic transformation occurs and cools down the material (Stage 3 to Stage 4). (iv) The cooled material absorbs heat from the ambient and thereby is heated up to room temperature (Stage 4 to Stage 1). This step can realize solid-state cooling. Actually, elastocaloric materials in cooling/heat-pumping devices can also undergo other thermodynamic cycles like Ericsson, Stirling, or a hybrid of them [6,41].

2.2. Characterization methods of elastocaloric effect (eCE)

The eCE manifested as isothermal entropy variation (ΔS_{iso}) or adiabatic temperature change (ΔT_{ad}) is usually characterized by direct or indirect methods. ΔT_{ad} is often measured directly by thermocouples welded on the materials. However, considering the inhomogeneity of the temperature field of most elastocaloric materials [42], a dense arrangement of monitoring points is required to ensure authenticity and thereby increasing the complexity of measurement. As an alternative, the non-contact infrared thermography with high frequency, simple operation and high accuracy can record the real-time full-field temperature evolution, enabling *in-situ* multi-field investigations of elastocaloric cooling [18,42]. Noticed that ΔT_{ad} should be measured under an adiabatic condition (i.e., the loading time $t_p \ll$ the heat transfer time t_h) [43]. ΔS_{iso} of stress-free materials can be determined directly by differential scanning calorimeter (DSC) technique, but the measured ΔS_{iso} usually is overestimated for the stress-induced martensitic

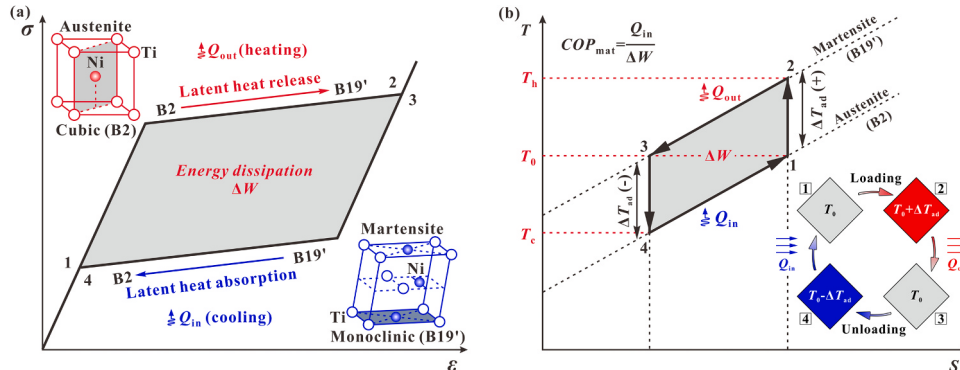


Fig. 1. Illustration of the elastocaloric effect in superelastic NiTi. (a) The stress-strain (σ - ϵ) curve and (b) the corresponding temperature-entropy (T - S) diagram (adapted from [18]).

transformation [44]. Generally, the stress-induced ΔS_{iso} from the typical first-order martensitic transformation in SMAs can be approximated by the Clausius-Clapeyron equation [45]:

$$\Delta S_{\text{iso}}(0 \rightarrow \sigma) = -\Delta \varepsilon^T (\text{d}\sigma^T / \text{dT}) \quad (1)$$

The corresponding theoretical adiabatic temperature change (ΔT_{ad}) is expressed as follows:

$$\Delta T_{\text{ad}} = -T \Delta S_{\text{iso}} / C_p \quad (2)$$

where $\Delta \varepsilon^T$, σ^T , T and C_p are transformation strain, critical transformation stress, ambient temperature and specific heat capacity, respectively. It should be noticed that the intrinsic hysteresis dissipation and the heat exchange might make the measured ΔT_{ad} slightly different from the theoretical value [12,16].

The coefficient of performance (COP_{mat}) is another key index to evaluate the cooling performance of elastocaloric materials. The COP_{mat} can be defined as cooling capacity (Q) divided by input work (ΔW) [46]:

$$COP_{\text{mat}} = Q / \Delta W \quad (3)$$

where Q is the extracted latent heat and ΔW is the stress-strain hysteresis loop area. From Eq. (3) it is clearly seen that enhanced caloric effect Q and reduced transformation hysteresis dissipation ΔW are beneficial to improve the efficacy of materials (COP_{mat}). Nevertheless, the strengthening of one index between Q and ΔW is normally at the expense of another one [47], indicating that sustained efforts for material optimization and development are still needed.

3. Elastocaloric effect (eCE) of traditional SMAs

3.1. The eCE of NiTi-based SMAs

3.1.1. Origin and cooling capacity of NiTi-based SMAs

The binary NiTi alloy was originally uncovered in 1959 from Naval Ordnance Laboratory and immediately attracted widespread attention owing to the unique superelasticity and shape memory effect [48]. Since then more diversified NiTi-based alloys were gradually developed [49–51]. Compared with the well-established theories and extensive applications in the fields of aeronautics and aerospace engineering, microelectronics, and biomedicine [52], NiTi-based SMAs are only beginning to show the potential in solid-state cooling. The large eCE of NiTi with a ΔT_{ad} of -14 K and a COP_{mat} of 12.6 was first demonstrated by Quarini and Prince in 2004 [40]. Subsequently, Cui et al. showed a great ΔT_{ad} of -17 K and a high COP_{mat} of 11.8 in the NiTi wire with a diameter of 3 mm [53]. In 2015, Pataky et al. revealed that a large ΔT_{ad}

of -14 K was achieved in the NiTi alloy when a tensile stress of ~ 500 MPa was applied along the crystallographic direction of [1 4 8] [54]. In addition, a giant ΔT_{ad} of ~ 30 K of NiTi was reported [2,19,55,56]. Noticed that the above large cooling capacity are readily available from ordinary NiTi and the latent heat of the material could be potentially increased by heat treatment, or adding elements to NiTi matrix [50]. Hence, NiTi-based SMAs possess a considerable cooling capacity.

3.1.2. Strategies toward enhanced cyclic stability of the eCE of NiTi-based SMAs

The cyclic stability of the eCE is of great significance for practical cooling in which refrigerants need to operate repeatedly and reversibly. However, the poor fatigue performance of conventional NiTi substantially prevents its wide industrial application as a refrigerant [18,57]. So far, extensive fruitful efforts have been dedicated to improving the cyclic stability of the eCE of NiTi-based SMAs [15,57–60]. Tušek et al. reported a ΔT_{ad} of -8 K with durable operation of 1×10^5 cycles at a strain amplitude of 1% for the NiTi plates with an initial pre-strain of 10% [57]. Recently, Chen et al. [18] shows a significantly improved cyclability of the eCE of NiTi by introducing gradient-grained structures (Fig. 2). The above improved cyclic stability of the eCE is achieved by microstructure control. Besides, the doping element also provides a viable strategy for enhancing the cyclic stability of the NiTi SMA [59]. Specifically, Cu-doping brings remarkable improvements in both stress-strain response and cyclic stability of the eCE of the NiTi alloy [60] (Fig. 3). However, it is should be noticed that Cu-doping leads to an obvious increase of critical transformation temperature, which is not favorable to cryogenic cooling applications. In fact, the determination of doping elements is also a huge system engineering. Schmidt et al. [61] studied more than 70 elements and finally doped Cu and V elements into the binary NiTi. The synthesized quaternary NiTiCuV alloy shows a ΔT_{ad} of -8 K with a good cyclic stability under a stress of ~ 550 MPa. More notably, the $\text{Ni}_{50.5}\text{Ti}_{49.1}\text{Fe}_{0.4}$ alloy fabricated by combining doping element and heat treatment possesses a giant ΔT_{ad} of -17 K and an improved fatigue property under a stress of ~ 500 MPa [62]. Not coincidentally, Chen et al. [63] obtained a large ΔT_{ad} of -17 K without obvious degradation after 5000 cycles by adding Cu and Al elements and subsequent grain refinement. Thus, it can be concluded that the combination of multiple strategies could be a promising approach to enhance the fatigue resistance of SMAs. In addition, precipitates are also beneficial to elevate the functional durability of elastocaloric materials by reducing the lattice mismatch between transforming phases [15,44,59]. The Cu-doped NiTi alloy, that is the $\text{Ti}_{54}\text{Ni}_{34}\text{Cu}_{12}$ film with the Ti_2Cu precipitate, shows a small lattice mismatch during B2-B19 transformation and thus brings an ultra-high fatigue life ($> 1 \times 10^7$

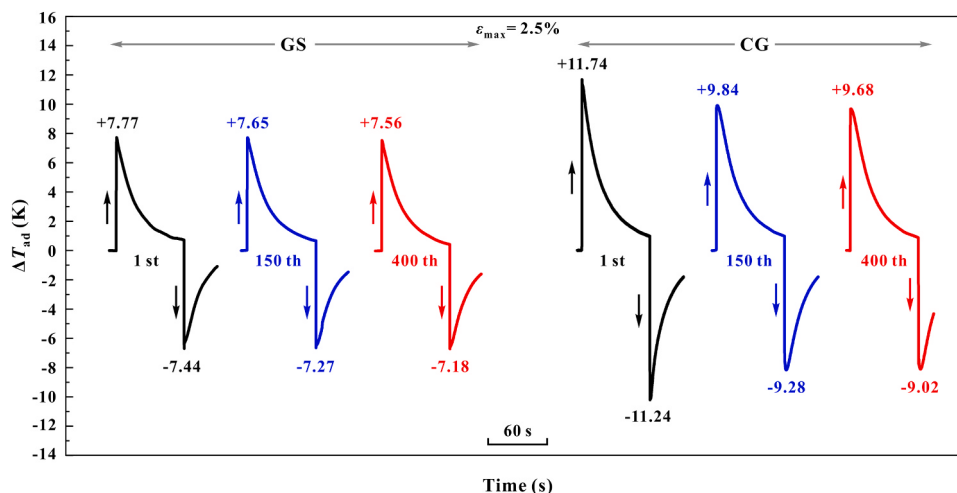


Fig. 2. Cyclic stability of elastocaloric effects of the gradient-structured (GS) and the homogeneous coarse-grained (CG) NiTi [18].

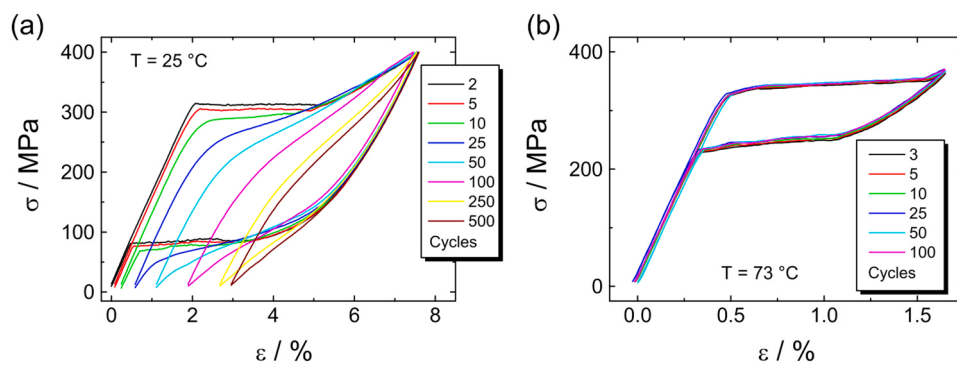


Fig. 3. Functional fatigue in superelastic NiTi-based films at low strain rates of 10^{-2} /min. (a) Binary NiTi and (b) NiTiCu [60].

cycles) [59]. Recently, Hou et al. demonstrated that the additive manufactured NiTi with Ni_3Ti precipitate has low hysteresis, excellent durability and high efficiency in refrigeration, opening up a novel pathway to develop advanced elastocaloric materials [15]. However, it should be noticed that the improved fatigue performance from the non-transformable precipitate phases (Ti_2Cu , NiTi_2 and Ni_3Ti) might compromise with the cooling capacity (latent heat) of elastocaloric materials.

3.1.3. Advances in broadening the working temperature window the eCE of NiTi-based SMAs

A broad working temperature window (WTW) is particularly desired for advanced elastocaloric materials, since the solid-state refrigerant may serve at high- or low-temperature conditions in practical applications. However, the effective WTW of traditional NiTi-based SMAs is usually less than 30 K due to the sharp first-order martensitic transformation [64]. To overcome the above shortcoming, Li et al. introduced large lattice distortions in the synthesized $\text{NiCuTiHf}_{0.6}\text{Zr}_{0.4}$ alloy to increase the material strength while reducing the temperature hysteresis, thus bringing a wide WTW [65]. Chen et al. [66] reported a Ti-44Ni-5Cu-1Al alloy with a large WTW exceeding 200 K through a combination of hot rolling and cold rolling (Fig. 4). The improved temperature stability of Ti-44Ni-5Cu-1Al is attributed to the abundant grain boundaries and defects, which significantly suppress the growth of martensite and therefore lead to a broad temperature window. Recently, Ahadi et al. [67] revealed an unprecedented eCE of nanocrystalline NiTi at ultra-low temperatures, in which the ΔT_{ad} reaches a large value of + 3.4 K after unloading at an ambient temperature of 18 K. The above anomalous phenomenon indicates that the eCE of the superelastic

nanocrystalline NiTi originates from the entropy change from elastic deformation at an ultra-low ambient temperature below the transformation range. Hitherto, systematic experimental data on the possible strategies to broaden WTW of NiTi-based SMAs are still not available.

3.1.4. Advances in overcoming the eCE heterogeneity of NiTi-based SMAs

Apart from large cooling capacity and efficiency, excellent durability, and wide WTW, the uniform temperature distribution is desired for NiTi-based SMAs as refrigerants. For the conventional coarse-grained superelastic NiTi SMA, the inhomogeneous behavior of the first-order transformation causes localized higher temperature Lüders-like bands [62,68], which will reduce the cooling efficiency of materials [12,68]. As an attempt to solve this problem, Chen et al. fabricated a nanocrystalline Ti-44Ni-5Cu-1Al alloy with spatial homogeneous strain and temperature fields due to the diffuse martensitic transformation [16]. Recently, Chen et al. achieved a rather spatially uniform temperature distribution in the gradient-structured NiTi SMA with average grain sizes varying from ~ 10 nm to ~ 3500 nm [18]. Such homogeneous distribution of temperature originates from the gradient structure effect introduced by localized laser surface annealing on a severely-deformed substrate. Hence, homogenizing the temperature distribution of NiTi-based SMAs is a difficult but, in principle, soluble challenge. In summary, NiTi-based SMAs have great potential in elastocaloric cooling applications.

3.2. The eCE of Cu-based SMAs

In 1938, before the concept of shape memory effect was suggested, Greninger and Mooradian found that the martensite content in Cu-Zn and Cu-Sn alloys waxes and wanes with the fall and rise of temperature [69]. In the 1970s, Miura et al. [70,71] first detected the temperature variation of Cu-Au-Zn alloy under adiabatic loading, which opens up the field of research on the caloric effects of Cu-based SMAs. Soon afterwards, Rodriguez et al. captured a pronounced eCE in the β -CuAlNi single crystal, in which a ΔT_{ad} of 14 K is achieved by stress-induced β - β' martensitic transformation of the material [39]. Blooming research on elastocaloric cooling of Cu-based SMAs emerges after Mañosa et al. [72] systematically studied the entropy changes from the martensitic transformation of Cu-Zn-Al, Cu-Al-Ni, and Cu-Al-Be alloys. In 2008, Bonnot et al. [25] evaluated the cooling capacity of the Cu-Zn-Al single crystal at different temperatures by theoretical calculation. The maximum calculated martensitic ΔS was about -1.21 J/mol K and the corresponding theoretical ΔT_{ad} was up to -15 K. However, only -7 K of ΔT_{ad} was detected in the experiment [73], the difference of ΔT_{ad} between experiment and calculation might arise from the unavoidable heat loss and incomplete transformation. For the polycrystalline Cu-Zn-Al, -6 K of ΔT_{ad} was obtained [74], which is comparable to that of magnetocaloric materials [28] but is far from that (~ 30 K) of NiTi-based SMAs [19,55,56]. To enlarge the cooling capacity of Cu-based SMAs, Xu et al. [75] produced a columnar-grained $\text{Cu}_{71.5}\text{Al}_{17.5}\text{Mn}_{11}$ alloy by directional

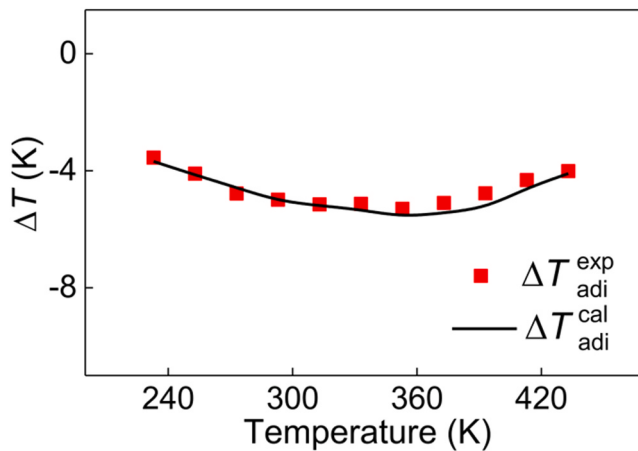


Fig. 4. Testing temperature dependence of the experimental adiabatic temperature change $\Delta T_{\text{ad}}^{\text{exp}}$ during the stress fast removing process (0.2 s^{-1}) from 1 GPa [66].

solidification, which possesses a large ΔT_{ad} of -13 K under low applied stress covering a wide WTW of more than 100 K. However, due to the intrinsically high brittleness of polycrystalline Cu-based SMAs, fatigue failure usually occurs during the training process [76]. For this reason, Bonnot et al. demonstrated that single crystal Cu-based SMAs could provide enhanced mechanical and cooling performances contrasted to polycrystal but generally at the expense of significantly improved cost and reduced bulk [25]. To overcome the high brittleness of the material, some fruitful attempts have been conducted [77–79]. In 2009, Xu et al. reported a liquid-phase (Taylor) wire forming process to dramatically improve the ductility and superelasticity (superelastic strain $\sim 6.8\%$) in the polycrystalline Cu-Al-Ni alloy [77]. Later on, Omori et al. [78] fabricated a bamboo-structured Cu-Al-Mn alloy with abnormally large grain sizes (~ 7 mm) by cyclic heat treatment. The Cu-Al-Mn alloy shows a high superelastic strain comparable to NiTi-based SMAs owing to the drastically decreased grain constraint. Noticed that the above work only focuses on the optimization of mechanical properties and neglects the eCE. Recently, Yuan et al. [79] investigated the eCE in Cu-Al-Mn SMA microwire produced by the Taylor-Ulitovsky method. The microwire with bamboo-like grain architecture exhibits a reversible ΔT_{ad} of -3.9 K with small hysteresis under a low driving stress of 150 MPa. After further multi-step cold-drawing [14], the Cu-Al-Mn microwire has favorable cyclic stability of eCE as shown in Fig. 5. From the viewpoint of material cost, driving force, heat conduction, and machinability, Cu-based SMAs are superior to the commonly used NiTi alloy [80]. However, some future work to improve the refrigeration capacity, superelasticity, and durability of Cu-based SMAs is necessary to enhance the elastocaloric cooling performances.

3.3. The eCE of Fe-based SMAs

Fe-based SMAs, used extensively as seismic damping materials and key connection components in civil and mechanical engineering [81], were originally discovered by Wayman in Fe-based precious alloys [82]. Nevertheless, due to the weak calorific effect arising from the semi- or non-thermal elastic martensitic transformation of Fe-based SMAs, their development and application in solid-state refrigeration are greatly limited. Thus far, the reported eCE of Fe-based SMAs is still scarce and mainly focuses on Fe-Rh-based and Fe-Pd-based SMAs. In 1992, Nikitin et al. [83] detected a ΔT_{ad} of -5.17 K from the stress-induced anti-ferromagnetism-ferromagnetism transformation of Fe-Rh alloy. Subsequently, Gràcia-Condal et al. [84] revealed that the stress-induced ΔT_{ad} of Fe₄₉Rh₅₁ is independent of the magnetic field, yet the phase transformation temperature of the material is closely related to the magnetic field. Therefore, the magnetic field can be used to regulate WTW of the material. Fe-Pd-based SMAs are also among the candidates of

elastocaloric materials. In 2013, Xiao et al. [85] first explored the eCE of the Fe-31.2 Pd single crystal, which shows a ΔT_{ad} of ~ 2 K under an applied stress of 100 MPa. Most noteworthy, the Fe-31.2 Pd single crystal has extremely low critical transformation stress and slim hysteresis under different ambient temperatures (Fig. 6), showing great potential in high-efficiency cooling. To enhance the cooling capacity of Fe-Pd alloys, Shen et al. [86] achieved an improved ΔT_{ad} of -5.4 K with a reduced critical transformation stress of 80 MPa in the Pd_{59.3}In_{23.2}Fe_{17.5} alloy with good superelastic behavior and ductility. In a word, Fe-based SMAs provide new ideas for the development of low-hysteresis, high-efficiency, and easy-to-drive refrigerants and also enrich the elastocaloric material system. If the challenges such as low cooling capacity, high cost and narrow WTW could be overcome, then Fe-based SMAs will have a bright future in elastocaloric cooling.

3.4. The eCE of ferromagnetic SMAs

3.4.1. Cooling capacity of ferromagnetic SMAs

Ferromagnetic SMAs combine the characteristics of ferromagnetic martensitic transformation (fast and remote actuation or sensing) and thermoelastic martensitic transformation (large recoverable strain) [87]. As a subgroup of SMAs with the nature of typical first-order martensitic transformation, their remarkable eCE is nowadays very active [88–90]. Ni-Mn-based SMAs are the earliest developed and most

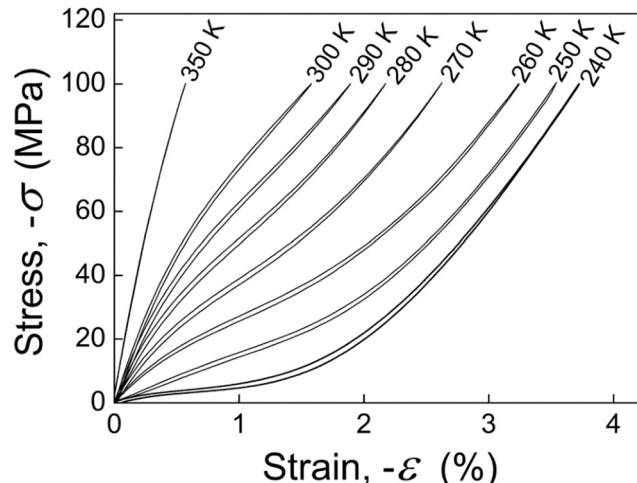


Fig. 6. Stress-strain curves of the Fe-Pd single crystal compressed in the [0 1]_P direction at stress of up to 100 MPa at various fixed temperatures [85].

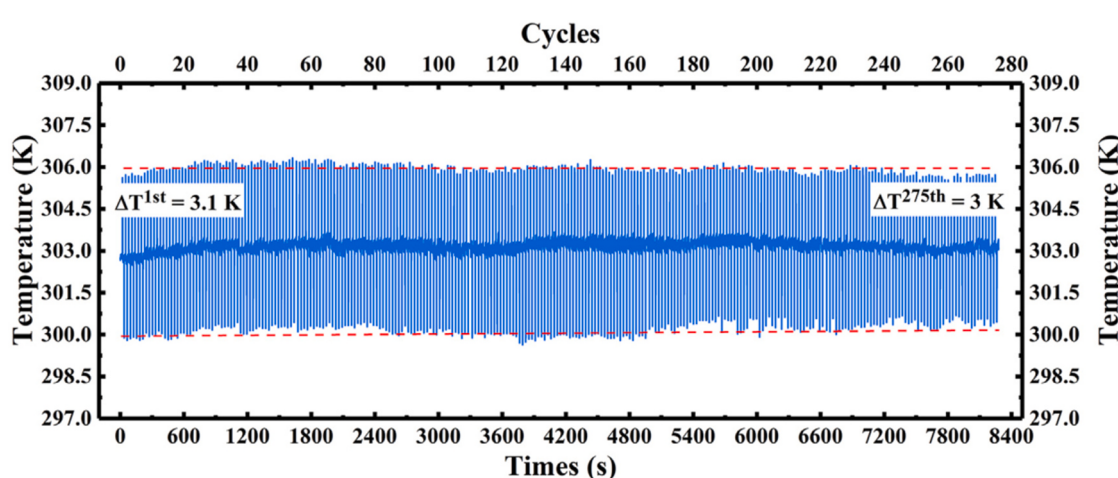


Fig. 5. Time dependence of the temperature change [14].

comprehensively studied ferromagnetic SMAs. Early reports on the eCE of ferromagnetic SMAs appeared in Ni-Mn-Ga alloys doped with Fe [91] and Co [92] elements. Fig. 7 shows the stress-induced entropy change of the Ni-Mn-Ga-Fe alloy as a function of temperature under given applied force. For the Ni-Mn-Ga-Co alloy, the magnetic field enhances the eCE, and the entropy change motivated by stress increases with the magnetic field (Fig. 8). Apparently, the small entropy change ($< 6 \text{ J kg}^{-1} \text{ K}^{-1}$) of the above materials is not sufficient for solid-state refrigeration applications. Hence, Huang et al. [93] improved both the entropy change and refrigeration capacity by increasing the atomic ordering in the Ni-Mn-Ga-Cu alloy. Moreover, a large ΔT_{ad} of -10.7 K is achieved from the stress-induced two-step structural transformation in the directionally solidified Ni₅₅Mn₁₈Ga₂₇ polycrystalline alloy with $< 111 >_A$ texture [94]. Recently, Cong et al. [17] reported a colossal eCE in the bulk polycrystalline Ni-Mn-Ti-B alloy with strikingly high values of ΔT_{ad} (-31.5 K) and ΔS_{iso} (-45 $\text{J kg}^{-1} \text{ K}^{-1}$), representing the highest values so far in ferromagnetic SMAs. The work inspires the discovery of giant caloric effects in a wide range of ferroelastic materials for solid-state cooling.

3.4.2. Strategies toward reduced brittleness and enhanced cyclic stability of ferromagnetic SMAs

High brittleness and poor cyclic stability originated from weak grain boundary cohesion of Ni-Mn-based SMAs are still vital issues to impede their long-term application [95,96]. For this reason, Yang et al. proposed a strategy of microalloying with boron to improve the cyclic stability of eCE of the (Ni_{51.5}Mn₃₃In_{15.5})_{99.7}B_{0.3} alloy, showing no degradation for more than 150 cycles [96]. Noticed that the eCE of the boron-free Ni_{51.5}Mn₃₃In_{15.5} degrades remarkably after only ~ 20 cycles [96]. Such enhanced cyclic stability of eCE mainly arises from the increased grain boundary cohesion and grain refinement due to microalloying with boron. Hot extrusion is also a feasible approach to improve the cyclic stability of the eCE of Ni-Mn-based SMAs. Specifically, the hot extruded Ni_{50.4}Mn_{27.3}Ga_{22.3} alloy with $< 111 >_A$ texture presents fine grains and low energy dissipation and thus shows more than 250 stable elastocaloric cycles without obvious degradation [97]. Recently, by optimizing the geometric compatibility at the interface between austenite and martensite of the Ni_{42.5}Fe_{1.0}Co_{6.5}Mn_{39.5}Sn_{10.5} alloy, the material exhibits high cyclic stability (> 2100 cycles) of eCE with a reversible ΔT_{ad} of -5 K as shown in Fig. 9 [98]. The aforementioned findings based on doping element, microalloying, introducing texture, microstructure control and compatibility regulation are of crucial importance for designing high-performance ferromagnetic materials for future solid-state cooling applications.

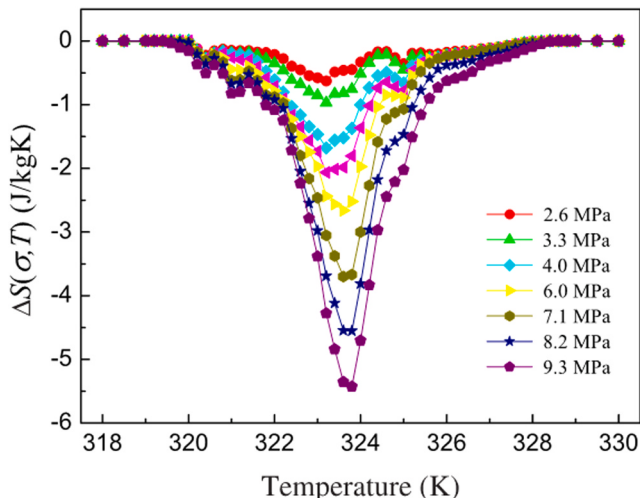


Fig. 7. Stress-induced changes of entropy as a function of temperature for selected values of the applied force [91].

3.5. Summary of the eCE of elastocaloric materials

3.5.1. Tips for designing elastocaloric materials with high eCE

In summary, the aforementioned available approaches might provide a reference for future sustained optimization and development of diverse elastocaloric materials. Specifically, the cooling capacity of the refrigerant is manifested as the exploitable latent heat which is proportional to the unit cell volume change across the phase transformation. Therefore, strategies such as heat treatment, microalloying or doping element could be employed to increase geometric differences between the crystal structures of the transforming phases and thus to enhance the cooling capacity of elastocaloric materials. Besides, a good mechanical property is the first precondition for sufficiently exploiting the latent heat of elastocaloric materials. From the perspective of application, the limited cyclic stability of eCE is still a major roadblock to the commercialization of elastocaloric cooling. The degradation of eCE mainly comes from the deformation mismatch between austenite and martensite during phase transformation. Hence, introducing self-accommodated structures such as compatible triplets, coherent phase boundaries, or multiphase nanocomposites by microalloying/doping element, magnetron sputtering, grain refinement or additive manufacturing could be a feasible avenue to improve the cyclic stability of the eCE. Noticed that a good lattice compatibility can bring an enhanced cyclic stability of the eCE, but in turn can reduce the cooling capacity of the elastocaloric materials. To overcome this issue, our preliminary results demonstrate that combination of multiple strategies is an effective route to achieve a compromise between these two opposing requirements [18]. Besides large cooling capacity and high cyclic stability, wide working temperature window and homogeneous eCE of the refrigerants are also particularly desired for an efficient active elastocaloric regenerator. Consequently, optimizing these two indices by introducing lattice distortions and other possible approaches deserves more attention.

3.5.2. Comparison in the eCE of elastocaloric materials

In addition to continuing to develop high-performance elastocaloric materials and perfecting the theoretical frameworks of solid-state refrigeration, how to select the appropriate elastocaloric materials as refrigerants according to the actual application requirements, environment, as well as specific refrigerators, is still not available. Hence, it is necessary to comprehensively identify the advantages and disadvantages of the numerous elastocaloric materials. NiTi-based SMAs possess great eCE, robust mechanical properties and mature theoretical models [44,99]. Fig. 10 shows a compilation of refrigeration performance data (i.e., $|\Delta T_{ad}|$ versus COP_{mat}) of various elastocaloric materials [20]. It is found that, from the perspective of both cooling capacity and efficiency of the refrigerant candidates, NiTi under compression mode is the front runner so far. However, the drawbacks such as large hysteresis, poor cyclic stability, high driving force, and undesirable machinability still greatly hinder the widespread commercialization of NiTi-based SMAs in elastocaloric cooling applications. For Cu-based SMAs, the driving force, heat conduction, and machinability are superior to the most NiTi-based alloys, but their cooling capacity, mechanical properties, and durability, which are more important than the performances mentioned above for the long-term service of refrigerants, are still far from those of NiTi-based SMAs. Fe-based SMAs have significant advantages in driving force and energy dissipation, yet the weak caloric effect, narrow transformation temperature interval, and high material cost put the material at a disadvantage among diverse elastocaloric materials. Ferromagnetic SMAs simultaneously possess the characteristics of ferromagnetic martensitic transformation and thermoelastic martensitic transformation as well as large caloric effect, which is favorable to multi-caloric cooling. Plenty of work to overcome the high brittleness and poor cyclic stability of ferromagnetic SMAs is essential to promote their widespread applications in solid-state cooling. Overall, NiTi-based SMAs are the most promising candidate as refrigerants among the

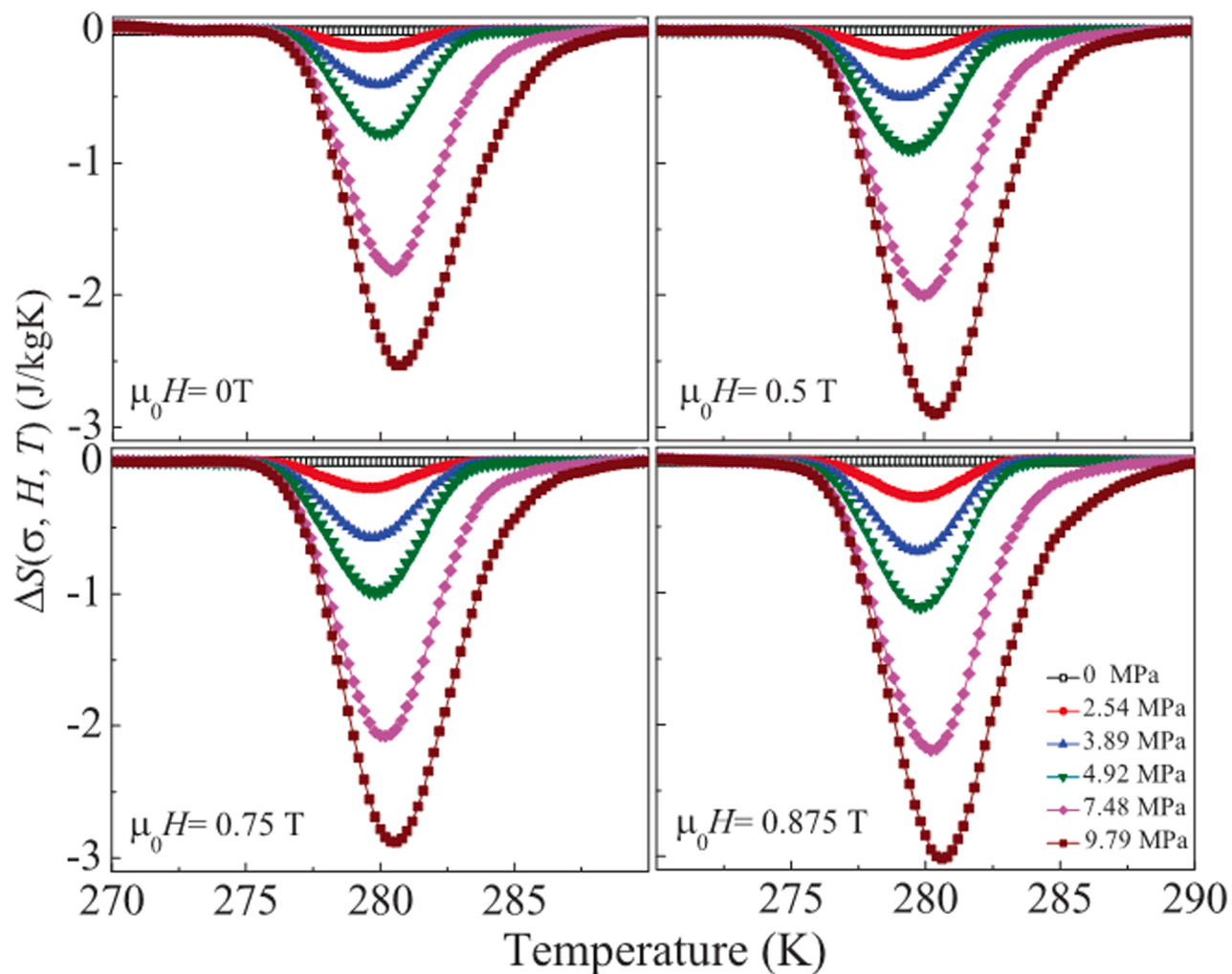


Fig. 8. Stress-induced entropy changes at different values of the stress and selected values of the applied magnetic field [92].

reported numerous elastocaloric materials.

4. State-of-the-art and challenges in developing elastocaloric devices

4.1. Prototypes

The development of elastocaloric devices is still in its infancy, and only a few cooling prototypes were reported around the world to-date [20,21]. As early as the 1970s, Banks [100] and Johnson [101] originally performed a simple heat engine design using elastocaloric materials, which provides a theoretical foundation for the subsequent development of refrigeration prototypes. In 1987, Shin et al. [102] proposed a synchronized twin crank design based on SMA coils, as shown in Fig. 11a. The coiled SMA wire is analogous to a spring, allowing for large strain and structural deformation, which can lead to more pronounced caloric effects. Saylor designed a tensile driven elastocaloric refrigeration prototype utilizing multiple NiTi wires (Fig. 11b) [103]. The tensile force of the prototype is provided by two non-parallel but synchronously rotating plates. The distance between the two plates on the right side at point B is slightly longer than that at point A. The NiTi wires are stretched to undergo forward transformation and release latent heat while moving toward point B, and the latent heat is taken away by passing air. After reaching point B, the wires on the other side subjected to reverse transformation associating with latent heat absorption, and the passing air can be cooled. Noticed that, the large

tensile force for inducing phase transformation of the NiTi wires is obtained by the rotation of the plates, thus bringing non-negligible friction. In addition, the slow heat exchange between air and NiTi wires greatly limits the operating frequency and thus reduces the output power of the system. In 2015, Qian et al. developed the world first compressive driven elastocaloric refrigeration prototype [104], in which two beds with multiple NiTi tubes were compressed by a motor driven screw-jack and the heat transfer is realized by the fluid water (Fig. 11c). As an optimization, Fig. 11d shows the second-generation compressive cooling prototype driven by hydraulic cylinders. This device consists of four beds with 37 NiTi tubes in each of them [23], compared to the first-generation prototype shown in Fig. 11c, it reduces the weight and the volume by 54% and 74% and increases the cooling capacity (65 W) four times. The major drawback of the aforementioned prototypes is the low cycling frequency (0.02–0.05 Hz), limited to the slow heat transfer. For this reason, Ossmer et al. [22] and Schmidt et al. [105] significantly improved the operating frequency (> 0.5 Hz) and efficiency of the refrigeration system through solid-solid conduction and increasing the contact area. In addition to the above single-stage elastocaloric devices, Tušek et al. [21] reported an active regenerator system consisting of nine parallel dog-bone shaped plates. The active cooling prototype can realize a temperature span of 15.3 K between the hot and cold sides using fluid water as a heat transfer medium. It is worthy to mention that the lifetime of the active cooling prototype is less than 6000 cycles [106] and the temperature span of the aforementioned elastocaloric devices is still far away from the adiabatic temperature change (~ 30 K) of the

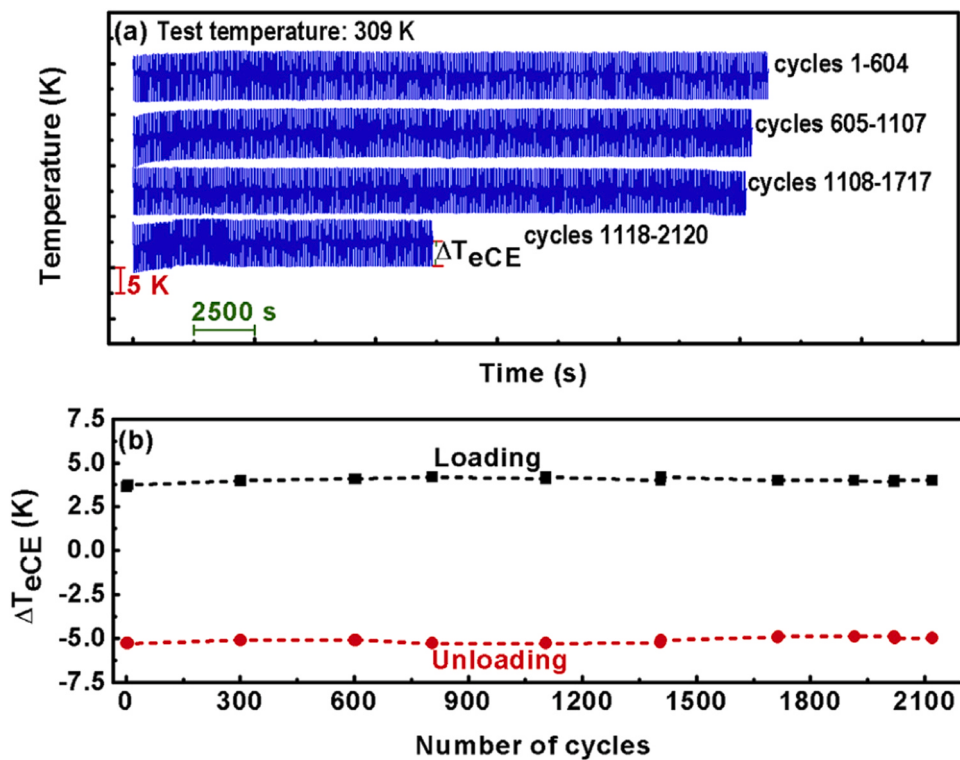


Fig. 9. (a) Cyclic temperature variation at 309 K shown as a function of time for the $\text{Ni}_{42.5}\text{Fe}_{1.0}\text{Co}_{6.5}\text{Mn}_{39.5}\text{Sn}_{10.5}$ alloy. The maximum applied stress was 350 MPa. The strain rates of $1.1 \times 10^{-2} \text{ s}^{-1}$ and 3.5 s^{-1} were used for loading and unloading, respectively. (b) Adiabatic temperature change ΔT_{eCE} deduced from (a), shown as a function of number of cycles [98].

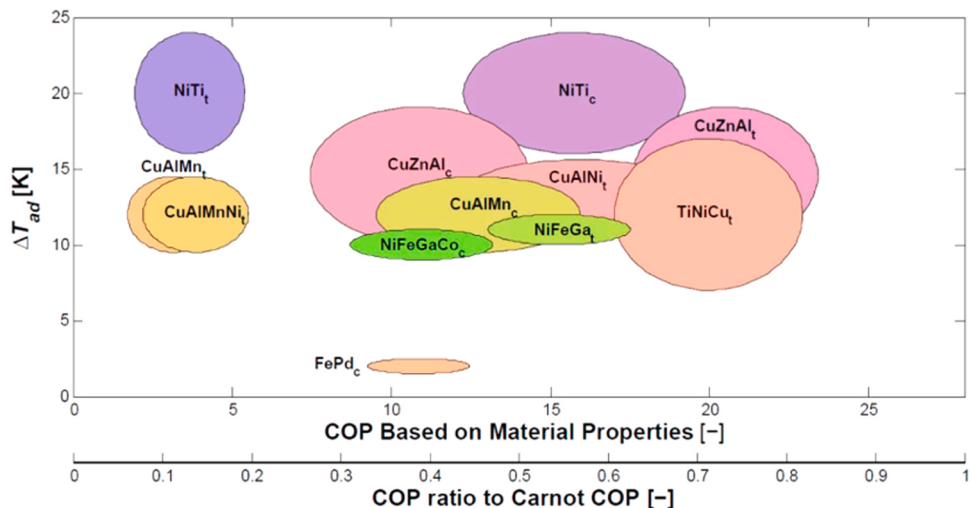


Fig. 10. Performance summary of elastocaloric materials ("t" means tension, and "c" stands for compression) [20].

NiTi alloy [2,19,55,56]. Cascaded systems or active regeneration might theoretically exceed the adiabatic temperature limit of the material [106,107], but there is still huge room for development and improvement in elastocaloric devices.

4.2. Challenges

The reported elastocaloric cooling prototypes are mainly based on the NiTi alloy, which shows great cooling potential and commercial value in solid-state refrigeration. As discussed in Sections 3.1 and 3.5, the desired properties like large latent heat and low hysteresis are generally mutually exclusive in NiTi-based SMAs, which is by far the

most intractable but crucial issue facing material scientists. To the best of our knowledge, synthesizing gradient microstructure is the only reported and effective strategy to overcome the above trade-off dilemma so far (Fig. 12) [18], showing a novel and viable method for developing high-performance elastocaloric materials. With that, we concluded that there is still considerable room for enhancement of eCE by optimizing the gradient microstructure. Besides, a compromise among the opposing requirements such as cooling capacity, efficiency, working temperature window, driving force, and durability also needs to be reached. Lifetime is another vital parameter for an elastocaloric cooling system. Take the NiTi refrigerant as an example, it has to endure up to 10^7 – 10^8 transformation cycles in a ten-year lifespan (assuming operation of six

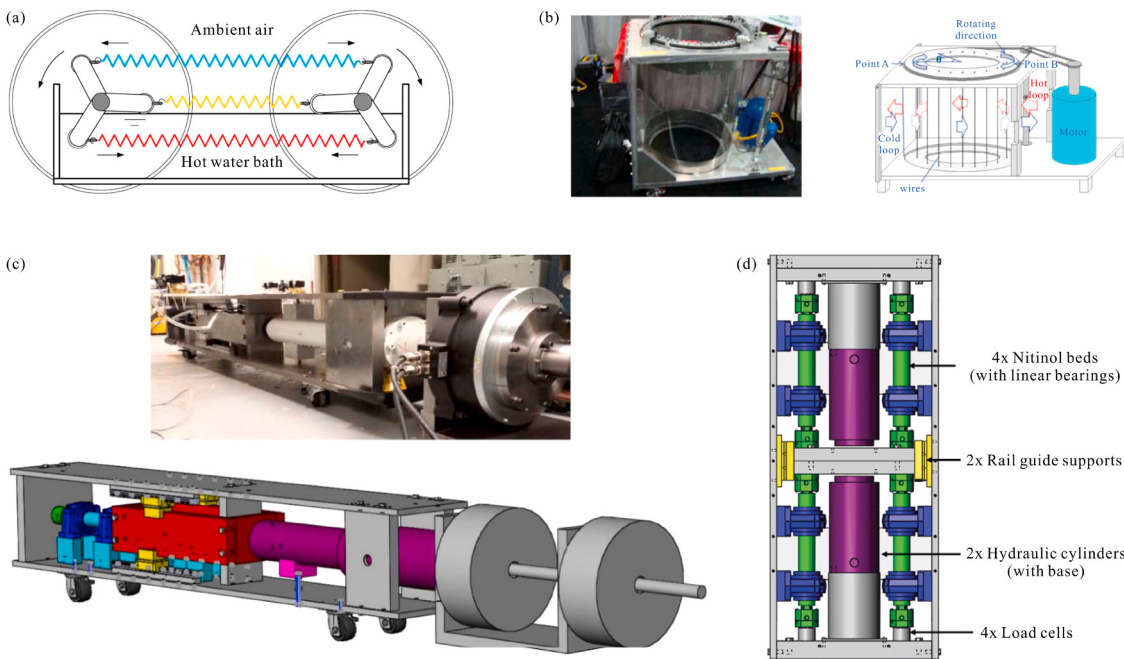


Fig. 11. Summary of a few typical elastocaloric devices. (a) Two pulleys design [102]. (b) NiTi wire based rotary prototype [103]. (c) University of Maryland, compression, NiTi tubes, driven by screw-jack [104]. (d) University of Maryland, compression, NiTi tubes, driven by hydraulic cylinders [23].

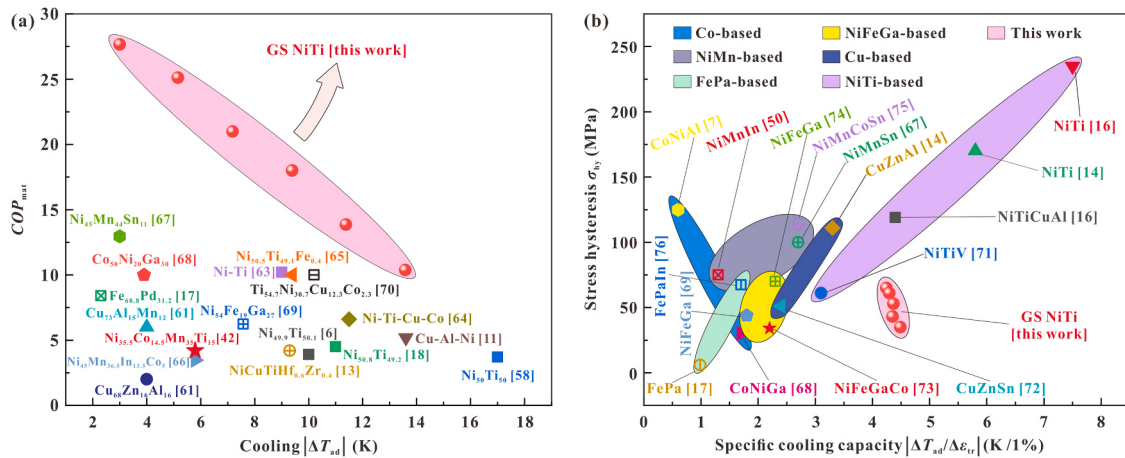


Fig. 12. Comparison of cooling performances between the gradient-structured (GS) NiTi and other elastocaloric materials [18].

months per year and half a day under 0.1–1 Hz) to confirm a reliable long-term operation of devices. Unfortunately, the fatigue life of bulk NiTi wires, plates, bars and tubes under tension or bending is only limited to 10^2 – 10^5 cycles with a catastrophic fracture [12,57,58],

[108–114], which is far away from the rigorous requirement of the cooling device. Our preliminary results demonstrate that the compressive NiTi cylinder exhibits an ultra-high fatigue life of ~ 70 million cycles and the COP_{mat} can achieve as high as 18.8 with an adiabatic

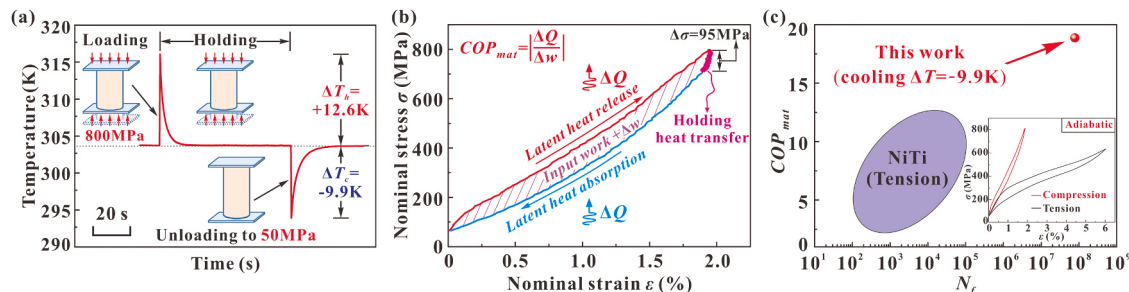


Fig. 13. (a) The temperature vs time curve and (b) the corresponding stress-strain response for the measurement of the coefficient of performance (COP_{mat}). (c) Comparison of COP_{mat} and the fatigue life (N_f) of NiTi between tensile and compressive working modes [43].

cooling temperature drop of 9.9 K (Fig. 13) [43], this is highly encouraging. In addition, the compressive cylinder still has a certain load carrying capacity after local spalling compared to the catastrophic fracture under tension or bending, showing excellent mechanical properties and structural stability. Overall, using the compressive working mode to drive the transformation of elastocaloric materials has the following advantages contrasted to other loading modes [2,15,19, 43,55,115]: (1) Achieve a more uniform macroscopic compressive stress and avoid stress concentration; (2) Significantly inhibit the initiation and growth of fatigue cracks and thus improve durability; (3) Good structural stability and system security manifested as obvious signs before failure and a certain load carrying capacity after local spalling. Besides, some comprehensive reviews on cyclic stability for SMAs are also reported elsewhere [116–118].

The driver is a crucial feature concerned with the regular operation of the refrigeration system, thereby an efficient and compact driver is the goal sought by designers. The driver used to induce transformation of solid-state materials in the elastocaloric devices is similar to the compressor in the vapor-compression refrigeration machine. However, the gaseous refrigerant in a vapor-compression system is usually compressed more than 200% of the specific volume, but the strain of the solid-state SMAs is only limited to 10%. As a result, the driver has to provide more than 20 times the external force to the solid-state SMAs so as to achieve the same input work in the gaseous refrigerant, while it needs to brake frequently to complete the heat transfer. Due to the stringent requirement and lack of consideration and development of elastocaloric actuators, there are still no drivers ideally fitted for the elastocaloric cooling applications nowadays. Table 2 summarizes potential drivers for elastocaloric devices in the future after optimizing the key indices such as force, displacement, cost, complexity and profile [20].

5. Summary

Elastocaloric cooling operated with green solid-state refrigerants offers an unprecedented opportunity to replace the conventional vapor-compression refrigeration technology with high global warming potential. In the past decades, elastocaloric materials and theoretical frameworks have been gradually enriched and improved, and refrigeration prototypes have also been designed and tested. We review the research progress and the opportunities and challenges of elastocaloric cooling, including the refrigeration fundamentals and the prototype design, and summarize them as follows:

- (1) Great caloric effect and robust mechanical properties make NiTi-based SMAs a front runner among the crowded elastocaloric materials for solid-state refrigeration. Further study based on doping element, microstructure control and crystallographic compatibility regulation to optimize the transformation hysteresis, durability, cooling efficiency and machinability is essential to accelerate their widespread application in elastocaloric cooling.
- (2) Cu-based SMAs have a low driving force, excellent heat conduction and machinability, but the cooling capacity, mechanical properties and durability, which are crucial for practical refrigeration applications, are still far from those of NiTi-based SMAs.
- (3) Fe-based SMAs show extremely low driving force and energy dissipation, yet the weak caloric effect, narrow working temperature interval, high cost are fatal in elastocaloric cooling.
- (4) Ferromagnetic SMAs combine the characteristics of ferromagnetic martensitic transformation and thermoelastic martensitic transformation as well as large latent heat, which are beneficial to multicaloric cooling. Considerable work to overcome their intrinsically high brittleness and poor cyclic stability is urgently needed.
- (5) A successful elastocaloric cooling prototype assembles elastocaloric materials, drivers, heat transfer systems, and the system

Table 2

Summary of different driver options for an elastocaloric cooling system [20].

Driver	Force	Displacement	Cost	Complexity	Profile
Pneumatic	0	+	+	+	-
Hydraulic	++	+	-	+	++
Linear motor	-	++	++	++	0
Screw-jack	++	+	-	0	-
Piezoelectric	+	-	+	+	-
Crankshaft	+	0	-	-	+

Zero means acceptable for a small scale prototype but should be improved. Minus means significant drawback. Plus means capable for large scale prototype. Double plus means better performance.

layout and thus requires the interdisciplinary cooperation of material scientists, physicists, engineers and mathematicians.

CRediT authorship contribution statement

Junyu Chen: Conceptualization, Methodology, Data curation, Writing – original draft. **Liping Lei:** Supervision, Resources, Funding acquisition, Writing – review & editing. **Gang Fang:** Project administration, Supervision, Writing – review & editing.

Declaration of Competing Interest

The authors declare that they have no known competing financial interests or personal relationships that could have appeared to influence the work reported in this paper.

Acknowledgments

This work was supported by the National Key Research and Development Program of China (No. 2017YFB0701801).

References

- [1] Z. Yang, D. Cong, Y. Yuan, R. Li, H. Zheng, X. Sun, Z. Nie, Y. Ren, Y. Wang, Large room-temperature elastocaloric effect in a bulk polycrystalline Ni-Ti-Cu-Co alloy with low isothermal stress hysteresis, *Appl. Mater. Today* 21 (2020) 682.
- [2] P. Kabirifar, A. Žerovnik, Ž. Ahćin, L. Porenta, M. Brojan, J. Tušek, P.K. A.Ž.Ž. Ahćin, L.P.M.B.J. Tušek, Elastocaloric cooling: state-of-the-art and future challenges in designing regenerative elastocaloric devices, *Stroj. Vestn.-J. Mech. E.* 65 (2019) 615–630.
- [3] Goetzler W., Zogg R., Young J., Johnson C., Energy savings potential and RD&D opportunities for non-vapor-compression HVAC technologies, prepared for U.S. Department of Energy (Navigant Consulting, Inc., 2014).
- [4] B. Li, Y. Kawakita, S. Ohira-Kawamura, T. Sugahara, H. Wang, J. Wang, Y. Chen, S.I. Kawaguchi, S. Kawaguchi, K. Ohara, Colossal barocaloric effects in plastic crystals, *Nature* 567 (7749) (2019) 506–510.
- [5] International Energy Agency. The Future of Cooling, Paris (<https://www.iea.org/reports/the-future-of-cooling>) (2018).
- [6] S. Qian, D. Nasuta, A. Rhoads, Y. Wang, Y. Geng, Y. Hwang, R. Radermacher, I. Takeuchi, Not-in-kind cooling technologies: a quantitative comparison of refrigerants and system performance, *Int. J. Refrig.* 62 (2016) 177–192.
- [7] S. Fähler, V.K. Pecharsky, Caloric effects in ferroic materials, *MRS Bull.* 43 (04) (2018) 264–268.
- [8] A. Kitanovski, J. Tušek, U. Tomc, U. Plazník, M. Ožbolt, A. Poredoš, Magnetocaloric energy conversion, green energy and technology, Springer International Publishing, Cham, Switzerland, 2015.
- [9] K. Gschneidner Jr., V.K. Pecharsky, Magnetocaloric materials, *Annu. Rev. Mater. Sci.* 30 (1) (2000) 387–429.
- [10] X. Hao, J. Zhai, L.B. Kong, Z. Xu, A comprehensive review on the progress of lead zirconate-based antiferroelectric materials, *Prog. Mater. Sci.* 63 (2014) 1–57.
- [11] L. Mañosa, D. Gonzalez-Alonso, A. Planes, M. Barrio, J.-L. Tamarit, I.S. Titov, M. Acet, A. Bhattacharyya, S. Majumdar, Inverse barocaloric effect in the giant magnetocaloric La-Fe-Si-Co compound, *Nat. Commun.* 2 (1) (2011) 1–5.
- [12] Y. Wu, E. Ertekin, H. Sehitoglu, Elastocaloric cooling capacity of shape memory alloys – role of deformation temperatures, mechanical cycling, stress hysteresis and inhomogeneity of transformation, *Acta Mater.* 135 (2017) 158–176.
- [13] D. Li, Z. Li, X. Zhang, B. Yang, D. Wang, X. Zhao, L. Zuo, Enhanced cyclability of elastocaloric effect in a directionally solidified Ni₅Mn₁₈Ga₂₆Ti₁ alloy with low hysteresis, *Scr. Mater.* 189 (2020) 78–83.
- [14] B. Yuan, M. Qian, X. Zhang, M. Imran, L. Geng, Enhanced cyclic stability of elastocaloric effect in oligocrystalline Cu-Al-Mn microwires via cold-drawing, *Int. J. Refrig.* 14 (2020) 54–61.

- [15] H. Hou, E. Simsek, T. Ma, N.S. Johnson, S. Qian, C. Cissé, D. Stasak, N. Al Hasan, L. Zhou, Y. Hwang, R. Radermacher, V.I. Levitas, M.J. Kramer, M.A. Zaeem, A. P. Stebner, R.T. Ott, J. Cui, I. Takeuchi, Fatigue-resistant high-performance elastocaloric materials made by additive manufacturing, *Science* 366 (6469) (2019) 1116–1121.
- [16] H. Chen, F. Xiao, X. Liang, Z. Li, Z. Li, X. Jin, T. Fukuda, Giant elastocaloric effect with wide temperature window in an Al-doped nanocrystalline Ti–Ni–Cu shape memory alloy, *Acta Mater.* 177 (2019) 169–177.
- [17] D. Cong, W. Xiong, A. Planes, Y. Ren, L. Mañosa, P. Cao, Z. Nie, X. Sun, Z. Yang, X. Hong, Colossal elastocaloric effect in ferroelastic Ni–Mn–Ti alloys, *Phys. Rev. Lett.* 122 (25) (2019), 255703.
- [18] J. Chen, L. Xing, G. Fang, L. Lei, W. Liu, Improved elastocaloric cooling performance in gradient-structured NiTi alloy processed by localized laser surface annealing, *Acta Mater.* 208 (2021), 116741.
- [19] L. Porenta, P. Kabirifar, A. Zerovnik, M. Čeborn, B. Žužek, M. Dolenc, M. Brojan, J. Tušek, Thin-walled Ni-Ti tubes under compression: ideal candidates for efficient and fatigue-resistant elastocaloric cooling, *Appl. Mater. Today* 20 (2020), 100712.
- [20] S. Qian, Y. Geng, Y. Wang, J. Ling, Y. Hwang, R. Radermacher, I. Takeuchi, J. Cui, A review of elastocaloric cooling: materials, cycles and system integrations, *Int. J. Refrig.* 64 (2016) 1–19.
- [21] J. Tušek, K. Engelbrecht, D. Eriksen, S. Dall’Olio, J. Tušek, N. Pryds, A regenerative elastocaloric heat pump, *Nat. Energy* 1 (2016) 16134.
- [22] H. Ossmer, F. Wendler, M. Gueltig, F. Lambrecht, S. Miyazaki, M. Kohl, Energy-efficient miniature-scale heat pumping based on shape memory alloys, *Smart Mater. Struct.* 25 (8) (2016), 085037.
- [23] S. Qian, Y. Geng, Y. Wang, J. Muehlbauer, J. Ling, Y. Hwang, R. Radermacher, I. Takeuchi, Design of a hydraulically driven compressive elastocaloric cooling system, *Sci. Technol. Built En.* 22 (5) (2016) 500–506.
- [24] H. Ossmer, F. Lambrecht, M. Gueltig, C. Chluba, E. Quandt, M. Kohl, Evolution of temperature profiles in TiNi films for elastocaloric cooling, *Acta Mater.* 81 (2014) 9–20.
- [25] R.R. Erell Bonnot, Lluís Mañosa, Eduard Vives, Antoni Planes, Elastocaloric effect associated with the martensitic transition in shape-memory alloys, *Phys. Rev. Lett.* 100 (12) (2008), 125901.
- [26] S.Y. Dan’Kov, A. Tishin, V. Pecharsky, K. Gschneidner, Magnetic phase transitions and the magnetothermal properties of gadolinium, *Phys. Rev. B* 57 (6) (1998) 3478–3490.
- [27] V.K. Pecharsky, K.A. Gschneidner Jr., Giant magnetocaloric effect in $Gd_5(Si_2Ge_2)$, *Phys. Rev. Lett.* 78 (23) (1997) 4494–4497.
- [28] K. Morrison, K. Sandeman, L. Cohen, C.P. Sasso, V. Basso, A. Barcza, M. Katter, J. Moore, K. Skokov, O. Gutfleisch, Evaluation of the reliability of the measurement of key magnetocaloric properties: a round robin study of La (Fe, Si, Mn) H₈ conducted by the SSEEC consortium of European laboratories, *Int. J. Refrig.* 35 (6) (2012) 1528–1536.
- [29] F. Guillou, G. Porcar, H. Yibole, N. van Dijk, E. Brück, Taming the first-order transition in giant magnetocaloric materials, *Adv. Mater.* 26 (17) (2014) 2671–2675.
- [30] P. Thacher, Electrocaloric effects in some ferroelectric and antiferroelectric Pb (Zr, Ti) O₃ compounds, *J. Appl. Phys.* 39 (4) (1968) 1996–2002.
- [31] X. Moya, S. Kar-Narayan, N.D. Mathur, Caloric materials near ferroic phase transitions, *Nat. Mater.* 13 (5) (2014) 439–450.
- [32] A.S. Mischenko, Q. Zhang, J.F. Scott, R.W. Whatmore, N.D. Mathur, Giant electrocaloric effect in thin-film PbZr_{0.95}Ti_{0.05}O₃, *Science* 311 (5765) (2006) 1270–1271.
- [33] S. Yuce, M. Barrio, B. Emre, E. Stern-Taulats, A. Planes, J.-L. Tamarit, Y. Mudryk, K.A. Gschneidner Jr., V.K. Pecharsky, L. Mañosa, Barocaloric effect in the magnetocaloric prototype $Gd_5Si_2Ge_2$, *Appl. Phys. Lett.* 101 (7) (2012), 071906.
- [34] P. Lloveras, E. Stern-Taulats, M. Barrio, J.-L. Tamarit, S. Crossley, W. Li, V. Pomjakushin, A. Planes, L. Mañosa, N. Mathur, Giant barocaloric effects at low pressure in ferrielectric ammonium sulphate, *Nat. Commun.* 6 (1) (2015) 1–6.
- [35] L. Manosa, D. Gonzalez-Alonso, A. Planes, E. Bonnot, M. Barrio, J.L. Tamarit, S. Aksoy, M. Acet, Giant solid-state barocaloric effect in the Ni–Mn–In magnetic shape-memory alloy, *Nat. Mater.* 9 (6) (2010) 478–481.
- [36] J. Gough, A description of a property of Caoutchouc, or Indian rubber, *Mem. Lit. Philos. Soc. Manch.* 1 (1805) 288–295.
- [37] W. Thomson, On the thermoelastic and thermomagnetic properties of matter, *Quart. J. Pure Appl. Math.* 1 (1857) 57–77.
- [38] J.P. Joule, On some thermo-dynamic properties of solids, *Philos. Trans. R. Soc. Lond.* 149 (1859) 91–131.
- [39] C. Rodriguez, L. Brown, The thermal effect due to stress-induced martensite formation in β -CuAlNi single crystals, *Metall. Mater. Trans. A* 11 (1) (1980) 147–150.
- [40] J. Quarini, A. Prince, Solid state refrigeration: cooling and refrigeration using crystalline phase changes in metal alloys, *Prog. Inst. Mech. Eng. Part C: J. Mech. Eng. Sci.* 218 (10) (2004) 1175–1179.
- [41] M. Schmidt, S.-M. Kirsch, S. Seelecke, A. Schütze, Elastocaloric cooling: from fundamental thermodynamics to solid state air conditioning, *Sci. Technol. Built Environ.* 22 (5) (2016) 475–488.
- [42] J. Chen, Y. Wu, H. Yin, In situ multi-field investigation of grain size effects on the rate-dependent thermomechanical responses of polycrystalline superelastic NiTi, *Mater. Lett.* 259 (2020), 126845.
- [43] J. Chen, K. Zhang, Q. Kan, H. Yin, Q. Sun, Ultra-high fatigue life of NiTi cylinders for compression-based elastocaloric cooling, *Appl. Phys. Lett.* 115 (9) (2019), 093902.
- [44] H. Hou, E. Simsek, D. Stasak, N.A. Hasan, S. Qian, R. Ott, J. Cui, I. Takeuchi, Elastocaloric cooling of additive manufactured shape memory alloys with large latent heat, *J. Phys. D: Appl. Phys.* 50 (40) (2017), 404001.
- [45] F. Xiao, T. Fukuda, X. Jin, J. Liu, T. Kakeshita, Elastocaloric effect associated with different types of martensitic transformations: typical first-order and weak first-order ones, *Phys. Status Solidi B* 255 (2) (2018), 1700246.
- [46] E.D.X. Moya, V. Heine, N.D. Mathur, Too cool to work, *Nat. Phys.* 11 (2015) 202–205.
- [47] A. Ahadi, Q. Sun, Stress hysteresis and temperature dependence of phase transition stress in nanostructured NiTi—Effects of grain size, *Appl. Phys. Lett.* 103 (2) (2013) 207–209.
- [48] W.J. Buehler, J. Gilfrich, R. Wiley, Effect of low-temperature phase changes on the mechanical properties of alloys near composition TiNi, *J. Appl. Phys.* 34 (5) (1963) 1475–1477.
- [49] K.N. Melton, O. Mercier, The mechanical properties of NiTi-based shape memory alloys, *Acta Metall.* 29 (2) (1981) 393–398.
- [50] J. Frenzel, A. Wieczorek, I. Opahle, B. Maab, R. Drautz, G. Eggeler, On the effect of alloy composition on martensite start temperatures and latent heats in Ni-Ti-based shape memory alloys, *Acta Mater.* 90 (2015) 213–231.
- [51] Z. Pu, D. Du, K. Wang, G. Liu, D. Zhang, X. Wang, B. Chang, Microstructure, phase transformation behavior and tensile superelasticity of NiTi shape memory alloys fabricated by the wire-based vacuum additive manufacturing, *Mater. Sci. Eng., A* 812 (2021), 141077.
- [52] J. Mohd Jani, M. Leary, A. Subic, M.A. Gibson, A review of shape memory alloy research, applications and opportunities, *Mater. Des.* 56 (2014) 1078–1113.
- [53] J. Cui, Y. Wu, J. Muehlbauer, Y. Hwang, R. Radermacher, S. Fackler, M. Wuttig, I. Takeuchi, Demonstration of high efficiency elastocaloric cooling with large ΔT using NiTi wires, *Appl. Phys. Lett.* 101 (7) (2012), 073904.
- [54] G.J. Pataky, E. Ertekin, H. Sehitoglu, Elastocaloric cooling potential of NiTi, Ni₂FeGa, and CoNiAl, *Acta Mater.* 96 (2015) 420–427.
- [55] K. Zhang, G. Kang, Q. Sun, High fatigue life and cooling efficiency of NiTi shape memory alloy under cyclic compression, *Scr. Mater.* 159 (2019) 62–67.
- [56] J.A. Shaw, S. Kyriakides, Thermomechanical aspects of NiTi, *J. Mech. Phys. Solids* 43 (8) (1995) 1243–1281.
- [57] J. Tušek, A. Žerovnik, M. Čeborn, M. Brojan, B. Žužek, K. Engelbrecht, A. Cadelli, Elastocaloric effect vs fatigue life: exploring the durability limits of Ni-Ti plates under pre-strain conditions for elastocaloric cooling, *Acta Mater.* 150 (2018) 295–307.
- [58] J. Tušek, K. Engelbrecht, L.P. Mikkelsen, N. Pryds, Elastocaloric effect of Ni-Ti wire for application in a cooling device, *J. Appl. Phys.* 117 (12) (2015), 124901.
- [59] C. Chluba, W. Ge, R. Lima de Miranda, J. Strobel, L. Kienle, E. Quandt, M. Wuttig, Ultralow-fatigue shape memory alloy films, *Science* 348 (6238) (2015) 1004–1007.
- [60] C. Bechtold, C. Chluba, R. Lima de Miranda, E. Quandt, High cyclic stability of the elastocaloric effect in sputtered TiNiCu shape memory films, *Appl. Phys. Lett.* 101 (9) (2012), 091903.
- [61] M. Schmidt, J. Ullrich, A. Wieczorek, J. Frenzel, A. Schütze, G. Eggeler, S. Seelecke, Thermal stabilization of NiTiCuV shape memory alloys: Observations during elastocaloric training, *Shap. Mem. Superelasticity* 1 (2) (2015) 132–141.
- [62] H. Ossmer, S. Miyazaki, M. Kohl, The elastocaloric effect in TiNi-based foils, *Mater. Today: Proc.* 2 (2015) S971–S974.
- [63] H. Chen, F. Xiao, X. Liang, Z. Li, X. Jin, T. Fukuda, Stable and large superelasticity and elastocaloric effect in nanocrystalline Ti-44Ni-5Cu-1Al (at%) alloy, *Acta Mater.* 158 (2018) 330–339.
- [64] S. Miyazaki, K. Otsuka, Y. Suzuki, Transformation pseudoelasticity and deformation behavior in a Ti-50.6 at% Ni alloy, *Scr. Metall.* 15 (3) (1981) 287–292.
- [65] S. Li, D. Cong, X. Sun, Y. Zhang, Z. Chen, Z. Nie, R. Li, F. Li, Y. Ren, Y. Wang, Wide-temperature-range perfect superelasticity and giant elastocaloric effect in a high entropy alloy, *Mater. Res. Lett.* 7 (12) (2019) 482–489.
- [66] H. Chen, F. Xiao, Z. Li, X. Jin, L. Mañosa, A. Planes, Elastocaloric effect with a broad temperature window and low energy loss in a nanograin Ti-44Ni-5Cu-1Al (at%) shape memory alloy, *Phys. Rev. Mater.* 5 (1) (2021), 015201.
- [67] A. Ahadi, T. Kawasaki, S. Harjo, W.-S. Ko, Q. Sun, K. Tsuchiya, Reversible elastocaloric effect at ultra-low temperatures in nanocrystalline shape memory alloys, *Acta Mater.* 165 (2019) 109–117.
- [68] H. Ossmer, C. Chluba, M. Gueltig, E. Quandt, M. Kohl, Local evolution of the elastocaloric effect in TiNi-based films, *Shap. Mem. Superelasticity* 1 (2) (2015) 142–152.
- [69] A.B. Greninger, V.G. Mooradian, Strain transformation in metastable beta copper-zinc and beta copper-tin alloys, *Trans. AIME* 128 (1938) 337–355.
- [70] S. Miura, S. Maeda, N. Nakanishi, Pseudoelasticity in Au-Cu-Zn thermoelastic martensites, *Philos. Mag.* 30 (3) (1974) 565–581.
- [71] S. Miura, Y. Morita, N. Nakanishi, Superelasticity and shape memory effect in Cu-Sn alloys, in: J. Perkins (Ed.), *Shape Memory Effects in Alloys*, Springer US, Boston, MA, 1975, pp. 389–405.
- [72] L. Mañosa, A. Planes, J. Ortín, B. Martínez, Entropy change of martensitic transformations in Cu-based shape-memory alloys, *Phys. Rev. B* 48 (6) (1993) 3611–3619.
- [73] E. Vives, S. Burrows, R.S. Edwards, S. Dixon, L. Mañosa, A. Planes, R. Romero, Temperature contour maps at the strain-induced martensitic transition of a Cu-Zn-Al shape-memory single crystal, *Appl. Phys. Lett.* 98 (1) (2011), 011902.
- [74] L. Mañosa, S. Jarque-Farnos, E. Vives, A. Planes, Large temperature span and giant refrigerant capacity in elastocaloric Cu-Zn-Al shape memory alloys, *Appl. Phys. Lett.* 103 (21) (2013), 211904.

- [75] S. Xu, H.-Y. Huang, J. Xie, S. Takekawa, X. Xu, T. Omori, R. Kainuma, Giant elastocaloric effect covering wide temperature range in columnar-grained Cu_{71.5}Al_{17.5}Mn₁₁ shape memory alloy, *APL Mater.* 4 (10) (2016), 106106.
- [76] S. Qian, Y. Geng, Y. Wang, T.E. Pillsbury, Y. Hada, Y. Yamaguchi, K. Fujimoto, Y. Hwang, R. Radermacher, J. Cui, Y. Yuki, K. Toyotake, I. Takeuchi, Elastocaloric effect in CuAlZn and CuAlMn shape memory alloys under compression, *Philos. Trans. A Math. Phys. Eng. Sci.* 374 (2074) (2016), 20150309.
- [77] Y. Chen, X. Zhang, D.C. Dunand, C.A. Schuh, Shape memory and superelasticity in polycrystalline Cu-Al-Ni microwires, *Appl. Phys. Lett.* 95 (17) (2009), 171906.
- [78] T. Omori, T. Kusama, S. Kawata, I. Ohnuma, Y. Sutou, Y. Araki, K. Ishida, R. Kainuma, Abnormal grain growth induced by cyclic heat treatment, *Science* 341 (6153) (2013) 1500–1502.
- [79] B. Yuan, X. Zhu, X. Zhang, M. Qian, Elastocaloric effect with small hysteresis in bamboo-grained Cu-Al-Mn microwires, *J. Mater. Sci.* 54 (13) (2019) 9613–9621.
- [80] Y. Araki, T. Endo, T. Omori, Y. Sutou, Y. Koetaka, R. Kainuma, K. Ishida, Potential of superelastic Cu-Al-Mn alloy bars for seismic applications, *Earthq. Eng. Struct. D* 40 (1) (2011) 107–115.
- [81] K. Li, Z. Dong, Y. Liu, L. Zhang, A newly developed Fe-based shape memory alloy suitable for smart civil engineering, *Smart Mater. Struct.* 22 (4) (2013), 045002.
- [82] C.M. Wayman, On memory effects related to martensite transformations and observations in β -brass and Fe₂Pt, *Scr. Metall.* 5 (6) (1971) 489–492.
- [83] S.A. Nikitin, G. Myalikgulyev, M.P. Annaorazov, A.L. Tyurin, R.W. Myndyev, S. A. Akopyan, Giant elastocaloric effect in FeRh alloy, *Phys. Lett. A* 171 (3) (1992) 234–236.
- [84] A. Gràcia-Condal, E. Stern-Taulats, A. Planes, L. Mañosa, Caloric response of Fe₄₉Rh₅₁ subjected to uniaxial load and magnetic field, *Phys. Rev. Mater.* 2 (8) (2018), 084413.
- [85] F. Xiao, T. Fukuda, T. Kakeshita, Significant elastocaloric effect in a Fe-31.2Pd (at.%) single crystal, *Appl. Phys. Lett.* 102 (16) (2013), 161914.
- [86] Q. Shen, D. Zhao, W. Sun, Z. Wei, J. liu, Microstructure, martensitic transformation and elastocaloric effect in Pd-In-Fe polycrystalline shape memory alloys, *Intermetallics* 100 (2018) 27–31.
- [87] E. Faran, D. Shilo, Ferromagnetic shape memory alloys—Challenges, applications, and experimental characterization, *Exp. Tech.* 40 (3) (2016) 1005–1031.
- [88] J. Liu, T. Gottschall, K.P. Skokov, J.D. Moore, O. Gutfleisch, Giant magnetocaloric effect driven by structural transitions, *Nat. Mater.* 11 (7) (2012) 620–626.
- [89] J. Liu, T.G. Woodcock, N. Scheerbaum, O. Gutfleisch, Influence of annealing on magnetic field-induced structural transformation and magnetocaloric effect in Ni-Mn-In-Co ribbons, *Acta Mater.* 57 (16) (2009) 4911–4920.
- [90] J. Marcos, A. Planes, L. Mañosa, F. Casanova, X. Batlle, A. Labarta, B. Martínez, Magnetic field induced entropy change and magnetoelasticity in Ni-Mn-Ga alloys, *Phys. Rev. B* 66 (22) (2002), 224413.
- [91] D.E. Soto-Parra, E. Vives, D. González-Alonso, L. Mañosa, A. Planes, R. Romero, J. A. Matutes-Aquino, R.A. Ochoa-Gamboa, H. Flores-Zúñiga, Stress- and magnetic field-induced entropy changes in Fe-doped Ni-Mn-Ga shape-memory alloys, *Appl. Phys. Lett.* 96 (7) (2010), 071912.
- [92] P.O. Castillo-Villa, D.E. Soto-Parra, J.A. Matutes-Aquino, R.A. Ochoa-Gamboa, A. Planes, L. Mañosa, D. González-Alonso, M. Stipcich, R. Romero, D. Ríos-Jara, Caloric effects induced by magnetic and mechanical fields in a Ni₅₀Mn₂₅–_xGa₂₅Co_x magnetic shape memory alloy, *Phys. Rev. B* 83 (17) (2011), 174109.
- [93] C. Huang, Y. Wang, Z. Tang, X. Liao, S. Yang, X. Song, Influence of atomic ordering on elastocaloric and magnetocaloric effects of a Ni-Cu-Mn-Ga ferromagnetic shape memory alloy, *J. Alloys Compd.* 630 (2015) 244–249.
- [94] D. Li, Z. Li, J. Yang, Z. Li, B. Yang, H. Yan, D. Wang, L. Hou, X. Li, Y. Zhang, C. Esling, X. Zhao, L. Zuo, Large elastocaloric effect driven by stress-induced two-step structural transformation in a directionally solidified Ni₅₅Mn₁₈Ga₂₇ alloy, *Scr. Mater.* 163 (2019) 116–120.
- [95] B. Lu, P. Zhang, Y. Xu, W. Sun, J. Liu, Elastocaloric effect in Ni₄₅Mn_{36.4}In_{13.6}Co₅ metamagnetic shape memory alloys under mechanical cycling, *Mater. Lett.* 148 (2015) 110–113.
- [96] Z. Yang, D.Y. Cong, X.M. Sun, Z.H. Nie, Y.D. Wang, Enhanced cyclability of elastocaloric effect in boron-microalloyed Ni-Mn-In magnetic shape memory alloys, *Acta Mater.* 127 (2017) 33–42.
- [97] L. Wei, X. Zhang, W. Gan, C. Ding, L. Geng, Hot extrusion approach to enhance the cyclic stability of elastocaloric effect in polycrystalline Ni-Mn-Ga alloys, *Scr. Mater.* 168 (2019) 28–32.
- [98] Y. Qu, A. Gràcia-Condal, L. Mañosa, A. Planes, D. Cong, Z. Nie, Y. Ren, Y. Wang, Outstanding calorific performances for energy-efficient multicaloric cooling in a Ni-Mn-based multifunctional alloy, *Acta Mater.* 177 (2019) 46–55.
- [99] Q.P. Sun, Y.J. He, A multiscale continuum model of the grain-size dependence of the stress hysteresis in shape memory alloy polycrystals, *Int. J. Solids Struct.* 45 (13) (2008) 3868–3896.
- [100] R. Banks, Energy conversion system. [based on use of memory metals], 1975.
- [101] A. Johnson, USA Patent No. US4055955 A, (1977).
- [102] M. Shin, C. Kim, Y. Chuang, K. Jee, USA Patent No. US4683721 A, (1987).
- [103] A. Saylor, ARPA-E summit technology showcase, 2012.
- [104] S. Qian, Y. Wu, J. Ling, J. Muehlbauer, Y. Hwang, I. Takeuchi, R. Radermacher, Design, development and testing of a compressive thermoelastic cooling prototype, *Int. Congr. Refrig.* (2015).
- [105] M. Schmidt, A. Schütze, S. Seelecke, Scientific test setup for investigation of shape memory alloy based elastocaloric cooling processes, *Int. J. Refrig.* 54 (2015) 88–97.
- [106] K. Engelbrecht, J. Tušek, D. Eriksen, T. Lei, C.-Y. Lee, J. Tušek, N. Pryds, A regenerative elastocaloric device: experimental results, *J. Phys. D: Appl. Phys.* 50 (42) (2017), 424006.
- [107] R. Snodgrass, D. Erickson, A multistage elastocaloric refrigerator and heat pump with 28 K temperature span, *Sci. Rep.* 9 (1) (2019) 1–10.
- [108] H. Sehitoglu, Y. Wu, E. Ertekin, Elastocaloric effects in the extreme, *Scr. Mater.* 148 (2018) 122–126.
- [109] K. Yan, P. Wei, F. Ren, W. He, Q. Sun, Enhance fatigue resistance of nanocrystalline NiTi by laser shock peening, *Shap. Mem. Superelasticity* 5 (4) (2019) 436–443.
- [110] H. Yin, Y. He, Z. Moumni, Q. Sun, Effects of grain size on tensile fatigue life of nanostructured NiTi shape memory alloy, *Int. J. Fatigue* 88 (2016) 166–177.
- [111] L. Zheng, Y. He, Z. Moumni, Lüders-like band front motion and fatigue life of pseudoelastic polycrystalline NiTi shape memory alloy, *Scr. Mater.* 123 (2016) 46–50.
- [112] C. Maletta, E. Sgambiterra, F. Furgiuele, R. Casati, A. Tuissi, Fatigue properties of a pseudoelastic NiTi alloy: strain ratcheting and hysteresis under cyclic tensile loading, *Int. J. Fatigue* 66 (2014) 78–85.
- [113] J. Chen, H. Yin, Q. Sun, Effects of grain size on fatigue crack growth behaviors of nanocrystalline superelastic NiTi shape memory alloys, *Acta Mater.* 195 (2020) 141–150.
- [114] J. Chen, Q. Kan, Q. Li, H. Yin, Effects of grain size on acoustic emission of nanocrystalline superelastic NiTi shape memory alloys during fatigue crack growth, *Mater. Lett.* 252 (2019) 300–303.
- [115] H. Hou, J. Cui, S. Qian, D. Catalini, Y. Hwang, R. Radermacher, I. Takeuchi, Overcoming fatigue through compression for advanced elastocaloric cooling, *MRS Bull.* 43 (04) (2018) 285–290.
- [116] A.R. Pelton, Nitinol fatigue: a review of microstructures and mechanisms, *J. Mater. Eng. Perform.* 20 (4–5) (2011) 613–617.
- [117] M. Imran, X. Zhang, Recent developments on the cyclic stability in elastocaloric materials, *Mater. Des.* 195 (2020), 109030.
- [118] M.J. Mahtabi, N. Shamsaei, M.R. Mitchell, Fatigue of nitinol: the state-of-the-art and ongoing challenges, *J. Mech. Behav. Biomed. Mater.* 50 (2015) 228–254.